New Phytologist

Tree height and leaf drought tolerance traits shape growth responses across droughts in a temperate broadleaf forest

Journal:	*New Phytologist*
Manuscript ID	NPH-MS-2020-34010
Manuscript Type:	MS - Regular Manuscript
Date Submitted by the Author:	24-Jul-2020
Complete List of Authors:	McGregor, Ian; Smithsonian Conservation Biology Institute, Conservation Ecology Center; North Carolina State University, Center for Geospatial Analytics Helcoski, Ryan; Smithsonian Conservation Biology Institute, Conservation Ecology Center Kunert, Norbert; Smithsonian Conservation Biology Institute, Conservation Ecology Center; Smithsonian Tropical Research Institute, Center for Tropical Forest Science Tepley, Alan; Smithsonian Conservation Biology Institute, Conservation Ecology Center Gonzalez-Akre, Erika; Smithsonian Conservation Biology Institute, Conservation Ecology Center Herrmann, Valentine; Smithsonian Conservation Biology Institute, Conservation Ecology Center Zailaa, Joseph; Smithsonian Conservation Biology Institute, Conservation Ecology Center; California State University Los Angeles, Biological Sciences Department Stovall, Atticus; Smithsonian Conservation Biology Institute, Conservation Ecology Center; University of Virginia, Department of Environmental Sciences; NASA Goddard Space Flight Center, Biospheric Sciences Bourg, Norman; Smithsonian Conservation Biology Institute, Conservation Ecology Center McShea, William; Smithsonian Conservation Biology Institute, Conservation Ecology Center Pederson, Neil; Harvard University, Harvard Forest Sack, Lawren; UCLA, Ecology and Evolutionary Biology; Anderson-Teixeira, Kristina; Smithsonian Conservation Biology Institute, Conservation Ecology Center; Smithsonian Tropical Research Institute, Center for Tropical Forest Science
Key Words:	annual growth, drought, Forest Global Earth Observatory (ForestGEO), temperate broadleaf deciduous forest, tree height, tree-ring, crown exposure, leaf drought tolerance traits

Title: Tree height and leaf drought tolerance traits shape growth responses across droughts in a temperate broadleaf forest

Authors: Ian R. McGregor[1,2], Ryan Helcoski[1], Norbert Kunert[1,3], Alan J. Tepley[1,4], Erika B. Gonzalez-Akre[1], Valentine Herrmann[1], Joseph Zailaa[1,5], Atticus E.L. Stovall[1,6,7], Norman A. Bourg[1], William J. McShea[1], Neil Pederson[8], Lawren Sack[9,10], Kristina J. Anderson-Teixeira[1,3]*

Author Affiliations:

1. Conservation Ecology Center; Smithsonian Conservation Biology Institute; National Zoological Park, Front Royal, VA 22630, USA
2. Center for Geospatial Analytics; North Carolina State University; Raleigh, NC 27607, USA
3. Center for Tropical Forest Science-Forest Global Earth Observatory; Smithsonian Tropical Research Institute; Panama, Republic of Panama
4. Canadian Forest Service, Northern Forestry Centre, Edmonton, Alberta, Canada
5. Biological Sciences Department; California State University; Los Angeles, CA 90032, USA
6. Department of Environmental Sciences, University of Virginia, Charlottesville, VA 22903, USA
7. NASA Goddard Space Flight Center; Greenbelt, MD 20771, USA
8. Harvard Forest, Petersham, MA 01366, USA
9. Department of Ecology and Evolutionary Biology; University of California, Los Angeles; Los Angeles, CA 90095, USA
10. Institute of the Environment and Sustainability; University of California, Los Angeles; Los Angeles, CA 90095, USA

*corresponding author: teixeirak@si.edu; +1 540 635 6546

Text	word count	other	n
Total word count (excluding summary, references and legends)	6,490	No. of figures	4 (all colour)
Summary	198	No. of Tables	3
Introduction	1,264	No of Supporting Information files	14
Materials and Methods	2,228		
Results	929		
Discussion	1927		
Acknowledgements	142		

Summary

- As climate change drives increased drought in many forested regions around the world, mechanistic understanding of the factors conferring drought resistance in trees is increasingly important. The dendrochronological record provides a window through which we can understand how tree size and species' traits shape growth responses during droughts.
- We analyzed tree-ring records for twelve species that comprise 97% of the woody productivity in a broadleaf deciduous forest of northern Virginia (USA) to test hypotheses on how tree height, microenvironment characteristics, and species' traits shaped drought responses across the three strongest regional droughts over a 60-year period (1950 - 2009).
- Individual-level drought resistance decreased with tree height, which was strongly correlated with exposure to higher evaporative demand and solar radiation. The potentially greater rooting volume of larger trees did not confer an advantage in sites with low topographic wetness index. Resistance was greater among species whose leaves experienced less shrinkage upon desiccation and lost turgor (wilted) at more negative water potentials.
- We conclude that tree height and leaf drought tolerance traits influence growth responses during drought, as recorded in the tree-ring record spanning historical droughts. Thus, these factors can be useful for predicting future drought responses under climate change.

Key words: annual growth; crown exposure; drought; Forest Global Earth Observatory (ForestGEO); leaf drought tolerance traits; temperate broadleaf deciduous forest; tree height; tree-ring

Introduction

Forests play a critical global role in climate regulation (Bonan, 2008), yet there remains enormous uncertainty as to how the forest-dominated terrestrial carbon sink will respond to climate change (Friedlingstein et al., 2006). An important aspect of this uncertainty lies with physiological responses of trees to drought (Kennedy et al., 2019). In many forested regions around the world, the risk of severe drought is increasing (Trenberth et al., 2014; Dai et al., 2018), often despite increasing precipitation (Intergovernmental Panel on Climate Change, 2015; Cook et al., 2015). Droughts, intensified by climate change, have been affecting forests worldwide and are expected to continue as one of the most important drivers of forest change in the future (Allen et al., 2010, 2015; McDowell et al., 2020). Understanding forest responses to drought requires elucidation of how tree size, microenvironment, and species' traits jointly influence individual-level drought resistance, defined here as a tree's ability to maintain growth during drought, and the extent to which their influence is consistent across droughts. Because the resistance and resilience (i.e., post-drought recovery) of growth to drought are linked to trees' probability of surviving drought (DeSoto et al., 2020; Liu et al., 2019), understanding growth responses can also help elucidate which trees are most vulnerable to drought-induced mortality. However, it has proven difficult to resolve the many factors affecting tree growth during drought with available forest census data, which only rarely captures extreme drought, and with tree-ring records, which capture multiple droughts but usually only sample a subset of a forest community, typically focusing on a single species or the largest individuals.

Many studies have shown that within and across species, large trees tend to be more affected by drought. Greater growth reductions for larger trees were first shown on a global scale by Bennett et al. (2015), and subsequent studies have reinforced this finding (*e.g.*, Hacket-Pain et al., 2016; Gillerot et al., 2020). It has yet to be resolved which of several potential underlying mechanisms most strongly shape these trends in drought response. First, tree height itself may be a primary driver. Taller trees face the biophysical challenge of lifting water greater distances against the effects of gravity and friction (McDowell et al., 2011; McDowell and Allen, 2015; Ryan et al., 2006; Couvreur et al., 2018). Vertical gradients in stem and leaf traits–including smaller and thicker leaves (higher leaf mass per area, LMA), greater resistance to hydraulic dysfunction (*i.e.*, more negative water potential at 50% loss of hydraulic conductivity, more negative P50), and lower hydraulic conductivity at greater heights (Couvreur et al., 2018; Koike et al., 2001; McDowell et al., 2011)–enable trees to become tall (Couvreur et al., 2018). Greater stem capacitance (*i.e.*, water storage capacity) of larger trees may also confer resistance to transient droughts (Phillips et al., 2003; Scholz et al., 2011). Indeed, tall trees require xylem of greater hydraulic efficiency, such that xylem conduit diameters are wider in the basal portions of taller trees, both within and across species (Olson et al., 2018; Liu et al., 2019), and throughout the conductive systems of angiosperms (Zach et al., 2010; Olson et al., 2014, 2018). Wider xylem conduits plausibly make large trees more vulnerable to embolism during drought (Olson et al., 2018), and traits conducive to efficient water transport may also lead to poor ability to recover from or re-route water around embolisms (Roskilly et al., 2019).

Larger trees may also have lower drought resistance because of microenvironmental and ecological factors. Their crowns tend to occupy more exposed canopy positions, which are associated with higher evaporative demand (Kunert et al., 2017). Subcanopy trees tend to fare better specifically due to the benefits of a buffered environment (Pretzsch et al., 2018). Counteracting the liabilities associated with tall height, large trees tend to have larger root systems (Enquist and Niklas, 2002), potentially mitigating some of the biophysical challenges they face by allowing greater access to water. Larger root systems–if they grant access

to deeper water sources–would be particularly advantageous in drier microenvironments (e.g., hilltops, as compared to valleys and streambeds) during drought. Finally, tree size-related responses to drought can be modified by species' traits and their distribution across size classes (Meakem et al., 2018; Liu et al., 2019). Understanding the mechanisms driving the greater relative growth reductions of larger trees during drought requires sorting out the interactive effects of height and associated exposure, root water access, and species' traits.

Debates have also arisen regarding the traits influencing tree growth responses to drought. Studies within temperate broadleaf forests have observed ring-porous species showing higher drought tolerance than diffuse-porous species (Friedrichs et al., 2009; Elliott et al., 2015; Kannenberg et al., 2019), but this distinction does not always hold (Martin-Benito and Pederson, 2015), would not hold in the global context (Wheeler et al., 2007; Olson et al., 2020) and does not resolve differences among the many species within each category. Commonly-measured traits including wood density and leaf mass per area (LMA) have been linked to drought responses within some temperate deciduous forests (Abrams, 1990; Guerfel et al., 2009; Hoffmann et al., 2011; Martin-Benito and Pederson, 2015) and across forests worldwide (Greenwood et al., 2017). However, in other cases these traits could not explain drought tolerance (e.g., in a tropical rainforest; Maréchaux et al., 2019), or the direction of response was not always consistent. For instance, higher wood density has been associated with greater drought resistance at a global scale (Greenwood et al., 2017), but correlated negatively with tree performance during drought in a broadleaf deciduous forest in the southeastern United States (Hoffmann et al., 2011). Thus, the perceived influence of these traits on drought resistance may actually reflect indirect correlations with other traits that more directly drive drought responses (Hoffmann et al., 2011).

In contrast, hydraulic traits have direct physiological linkages to tree growth and mortality responses to drought. For instance, water potentials at which percent the loss of conductivity surpasses a certain threshold (e.g., P50 and P88, representing 50 and 88% loss of conductivity, respectively) and hydraulic safety margin (*i.e.*, difference between typical minimum water potentials and P50 or P88) correlate with drought performance across global forests (Anderegg et al., 2016). However, these are time-consuming to measure and therefore infeasible for predicting or modeling drought responses in highly diverse forests (*e.g.*, in the tropics). More easily-measurable leaf drought tolerance traits that have direct linkage to plant hydraulic function can explain variation in plant distribution and function (Medeiros et al., 2019). These include leaf area shrinkage upon desiccation (PLA_{dry}; Scoffoni et al., 2014) and the leaf water potential at turgor loss point (π_{tlp}), *i.e.,* the water potential at which leaf wilting occurs (Bartlett et al., 2016a; Zhu et al., 2018). Both traits correlate with hydraulic vulnerability and drought tolerance as part of unified plant hydraulic systems (Scoffoni et al., 2014; Bartlett et al., 2016a; Zhu et al., 2018; Farrell et al., 2017). The abilities of both PLA_{dry} and π_{tlp} to explain tree drought resistance remains untested.

Here, we examine how tree height, microenvironment characteristics, and species' traits collectively shape drought resistance, defined as the ratio of annual growth in a drought year to that which would be expected in the absence of drought based on previous years' growth. We test a series of hypotheses and associated specific predictions (Table 1) based on the combination of tree-ring records from the three strongest droughts over a 60-year period (1950 - 2009), species trait measurements, and census and microenvironmental data from a large forest dynamics plot in Virginia, USA. First, we focus on how tree size, alone and in its interaction with microenvironmental gradients, influences drought resistance. We examine the contemporary relationship between tree height and microenvironment, including growing season meteorological conditions

and crown exposure. We then test whether, consistent with most forests globally, larger-diameter, taller trees tend to have lower drought resistance in this forest, which is in a region (eastern North America) represented by only two studies in the global review of (Bennett et al., 2015). We also test for an influence of potential access to available soil water, which should be greater for larger trees in dry but not in perpetually wet microsites. Finally, we focus on the role of species' traits, testing the hypothesis that species' traits-–particularly leaf drought tolerance traits-–predict drought resistance. We test predictions that drought resistance is higher in ring-porous than semi-ring and diffuse-porous species and that it is correlated with wood density–either positively (Greenwood et al., 2017) or negatively (Hoffmann et al., 2011) and positively correlated with LMA. We further test predictions that species with low PLA_{dry} have higher drought resistance, and that species whose leaves lose turgor lower water potentials (more negative π_{tlp}) have higher resistance.

Materials and Methods

Study site and microclimate

Research was conducted at the 25.6-ha ForestGEO (Forest Global Earth Observatory) study plot at the Smithsonian Conservation Biology Institute (SCBI) in Virginia, USA (38°53'36.6"N, 78°08'43.4"W; Fig. **S1**) (Bourg et al., 2013; Anderson-Teixeira et al., 2015a). SCBI is located in the central Appalachian Mountains near the northern boundary of Shenandoah National Park. Elevations range from 273 to 338 m above sea level with a topographic relief of 65m (Bourg et al., 2013). Climate is humid temperate, with mean annual temperature of 12.7°C and precipitation of 1005 mm yr^{-1} during our study period (1960-2009; source: CRU TS v.4.01; Harris et al., 2014). Dominant tree taxa within this secondary forest include *Liriodendron tulipifera*, oaks (*Quercus* spp.), and hickories (*Carya* spp.; Table 2).

Identifying drought years

We identified the three largest droughts within the time period 1950-2009, defining drought (Slette et al., 2019) as events with anomalously dry peak growing season climatic conditions. Specifically, we used the metric of Palmer Drought Severity Index (PDSI) during May-August (MJJA; Table S1), which were identified by Helcoski et al. (2019) as the months of the current year to which annual tree growth was most sensitive at this site. PDSI divisional data for Northern Virginia were obtained from NOAA (https://www7.ncdc.noaa.gov/CDO/CDODivisionalSelect.jsp) in December 2017. Based on this, we identified the three strongest droughts during the study period (Figs. **1, S1**; Table S1).

The droughts differed in intensity and antecedent moisture conditions (Fig. **S1**, Table S1). The 1966 drought was preceded by two years of moderate drought during the growing season and severe to extreme drought starting the previous fall. In August 1966, $PDSI$ reached its lowest monthly value (-4.82) of the three droughts. The 1977 drought was the least intense throughout the growing season, and it was preceded by 2.5 years of near-normal conditions, making it the mildest of the three droughts. The 1999 drought was preceded by wetter than average conditions until the previous June, but $PDSI$ plummeted below -3.0 in October 1998 and remained below this threshold through August 1999.

Data collection and preparation

Within or just outside the ForestGEO plot, we collected data on a suite of variables including tree heights, microenvironment characteristics, and species traits (Table 3). The SCBI ForestGEO plot was censused in

2008, 2013, and 2018 following standard ForestGEO protocols, whereby all free-standing woody stems $\geq$ 1cm diameter at breast height (DBH) were mapped, tagged, measured at DBH, and identified to species (Condit, 1998). From these census data, we used measurements of DBH from 2008 to calculate historical DBH and data for all stems $\geq$ 10cm to analyze functional trait composition relative to tree height (all analyses described below). Census data are available through the ForestGEO data portal (www.forestgeo.si.edu).

We analyzed tree-ring data (xylem growth increment) from 571 trees representing the twelve dominant species (Table 2; Fig. **S2**). Selected species were those with the greatest contributions to woody aboveground net primary productivity ($ANPP_{stem}$) and together comprised 97% of study plot $ANPP_{stem}$ between 2008 and 2013 (Helcoski et al., 2019). Cores (one per tree) were collected within the ForestGEO plot at breast height (1.3m) in 2010-2011 or 2016-2017. In 2010-2011, cores were collected from randomly selected live trees of each species that had at least 30 individuals $\geq$ 10 cm DBH (Bourg et al., 2013). Annual tree mortality censuses were initiated in 2014 (Gonzalez-Akre et al., 2016), and in 2016-2017, cores were collected from all trees found to have died since the previous year's census. We note that drought was probably not a cause of mortality for these trees, as monthly May-Aug $PDSI$ did not drop below -1.75 in these years or the three years prior (2013-2017), and that trees cored dead displayed similar climate sensitivity to trees cored live (Helcoski et al., 2019). Cores were sanded, measured, and crossdated using standard procedures, as detailed in (Helcoski et al., 2019). The resulting chronologies (Fig. **1a**) were published in Zenodo (DOI: 10.5281/zenodo.2649302) in association with Helcoski et al. (2019).

For each cored tree, we combined tree-ring records and allometric equations of bark thickness to reconstruct DBH for the years 1950-2009. Prior DBH was estimated using the following equation:

$$DBH_Y = DBH_{2008} - 2 * \left[r_{bark,2008} - r_{bark,Y} + \sum_{year=Y}^{2008} r_{ring,Y} \right]$$

Here, Y denotes the year of interest, r_{ring} denotes ring width derived from cores, and r_{bark} denotes bark thickness. Bark thickness was estimated from species-specific allometries based on the bark thickness data from the site (Anderson-Teixeira et al., 2015b). Specifically, we used linear regression on log-transformed data to relate r_{bark} to diameter inside bark from 2008 data (Table S2), which were then used to determine r_{bark} in the DBH reconstruction.

Tree heights (H) were measured by several researchers for a variety of purposes between 2012 and 2019 (n=1,518 trees). Methods included direct measurements using a collapsible measurement rod on small trees (NEON, 2018) or a tape measure on recently fallen trees (this study); geometric calculations using clinometer and tape measure (Stovall et al., 2018a) or digital rangefinders (Anderson-Teixeira et al., 2015b; NEON, 2018); and ground-based LiDAR (Stovall et al., 2018b). Rangefinders used either the tangent method (Impulse 200LR, TruPulse 360R) or the sine method (Nikon ForestryPro) for calculating heights. Both methods are associated with some error (Larjavaara and Muller-Landau, 2013), but in this instance there was no clear advantage of one or the other. Measurements from the National Ecological Observatory Network (NEON) were collected near the ForestGEO plot following standard NEON protocol, whereby vegetation of short stature was measured with a collapsible measurement rod, and taller trees with a rangefinder (NEON, 2018). Species-specific height allometries were developed (Table S3) using log-log regression ($ln[H] \sim ln[DBH]$). For species with insufficient height data to create reliable species-specific allometries (n=2, JUNI and FRAM), heights were calculated from an equation developed by combining the height

measurements across all species. We then used these allometries to estimate H for each drought year, Y, based on reconstructed DBH_Y. The distribution of H across drought years is shown in Fig. **S3**.

To characterize how environmental conditions vary with height, data were obtained from the NEON tower located <1km from the study area via the neonUtilities package (Lunch et al., 2020). We used wind speed, relative humidity, and air temperature data, all measured over a vertical profile spanning heights from 7.2 m to above the top of the tree canopy (31.0 or 51.8m, depending on censor), for the years 2016-2018 (NEON, 2018). After filtering for missing and outlier values, we determined the daily minima and maxima, which we then aggregated at the monthly scale.

Crown position–a categorical variable classifying trees based on exposure to sunlight–was recorded for all cored trees that remained standing during the growing season of 2018 following the protocol of Jennings et al. (1999). Trees were classified as follows: *dominant* trees were defined as those with crowns above the general level of the canopy, *co-dominant* trees as those with crowns within the the canopy; *intermediate* trees as those with crowns below the canopy level, but illuminated from above; and *suppressed* as those below the canopy and receiving minimal direct illumination from above.

Topographic wetness index (TWI), used here as a metric of long-term mean moisture availability, was calculated using the dynatopmodel package in R (Fig. **S2**) (Metcalfe et al., 2018). Originally developed by Beven and Kirkby (1979), TWI was part of a hydrological run-off model and has since been used for a number of purposes in hydrology and ecology (Sørensen et al., 2006). TWI calculation depends on an input of a digital elevation model (DEM; ~3.7 m resolution from the elevatr package (Hollister, 2018)), and from this yields a quantitative assessment defined by how "wet" an area is, based on areas where run-off is more likely. From our observations in the plot, TWI performed better at categorizing wet areas than the Euclidean distance from the stream.

Species' trait data were collected in August 2018 (Tables 2-3; Fig. **S4**). We sampled small, sun-exposed branches up to eight meters above the ground from three individuals of each species in and around the ForestGEO plot. Sampled branches were re-cut under water at least two nodes above the original cut and re-hydrated overnight in covered buckets under opaque plastic bags before measurements were taken. Rehydrated leaves taken towards the apical end of the branch (n=3 per individual: small, medium, and large) were scanned, weighed, dried at 60° C for $\geq$ 48 hours, and then re-scanned and weighed. Leaf area was calculated from scanned images using the LeafArea R package (Katabuchi, 2019). LMA was calculated as the ratio of leaf dry mass to fresh area. PLA_{dry} was calculated as the percent loss of area between fresh and dry leaves. Wood density was calculated for ~1cm diameter stem samples (bark and pith removed) as the ratio of dry weight to fresh volume, which was estimated using Archimedes' displacement. We used the rapid determination method of Bartlett et al. (2012) to estimate osmotic potential at turgor loss point (π_{tlp}). Briefly, two 4 mm diameter leaf discs were cut from each leaf, tightly wrapped in foil, submerged in liquid nitrogen, perforated 10-15 times with a dissection needle, and then measured using a vapor pressure osmometer (VAPRO 5520, Wescor, Logan, UT, USA). Osmotic potential (π_{osm}) given by the osmometer was used to estimate (π_{tlp}) using the equation $\pi_{tlp} = 0.832\pi_{osm}^{-0.631}$ (Bartlett et al., 2012).

Statistical Analysis

For each drought year, we calculated a metric drought resistance (Rt) as the ratio of basal area increment (BAI; *i.e.*, change in cross-sectional area) during the drought year to the mean BAI over the five years preceding the drought (Lloret et al., 2011). Thus, Rt values <1 and >1 indicate growth reductions and

increases, respectively. Because the Rt metric could be biased by directional pre-drought growth trends, we also tried an intervention time series analysis (ARIMA, Hyndman et al., 2020) that predicted mean drought-year growth based on trends over the preceding ten years and used this value in place of the five-year mean in calculations of resistance (Rt_{ARIMA}= observed BAI/ predicted BAI). The two metrics were strongly correlated (Fig. **S5**). Visual review of the individual tree-ring sequences with the largest discrepancies between these metrics revealed that Rt was less prone to unreasonable estimates than Rt_{ARIMA}, so we selected Rt as our focal metric, presenting parallel results for Rt_{ARIMA} in the Supplementary Info. In this study we focus exclusively on drought resistance metrics (Rt or Rt_{ARIMA}), and not on the resilience metrics described in Lloret et al. (2011), because (1) we would expect resilience to be controlled by a different set of mechanisms, and (2) the findings of DeSoto et al. (2020) suggest that Rt is a more important drought response metric for angiosperms in that low resistance to moderate droughts was a better predictor of mortality during subsequent severe droughts than the resilience metrics.

Analyses focused on testing the predictions presented in Table 1 with Rt as the response variable, and then repeated using Rt_{ARIMA} as the response variable. Models were run for all drought years combined and for each drought year individually. The general statistical model for hypothesis testing was a mixed effects model, implemented in the lme4 package in R (Bates et al., 2019). In the multi-year model, we included a random effect of tree nested within species and a fixed effect of drought year to represent the combined effects of differences in drought characteristics. Individual year models included a random effect of species. All models included fixed effects of independent variables of interest (Tables 1,3) as specified below. All variables across all best models had variance inflation factors <1.2 (1 +/- 0.019). We used AICc to assess model selection, and conditional/marginal R-squared to assess model fit as implemented in the AICcmodavg package in R (Mazerolle and portions of code contributed by Dan Linden., 2019). AICc refers to a corrected version of AICc, and is best suited for small data sizes (see Brewer et al., 2016).

To avoid over-fitting models with five species traits (Table 3) across only 12 species, we did not include all traits as fixed effects in a single linear mixed model, but rather conducted individual tests of each species trait to determine the relative importance and appropriateness for inclusion in the main model. These tests followed the model structure specified above, then added $ln[H]$ and $ln[TWI]$ to create a base model against which we tested traits. Trait variables were considered appropriate for inclusion in the main model if they had a consistent direction of response across all droughts and if their addition to the base model improved fit (at ΔAICc $\geq$ 1.0) in at least one drought year (Table S4). We note that we did not use the ΔAICc $\geq$ 1.0 criterion as a test of significance, but rather of whether the variable had enough influence to be considered as a *candidate* variable in full models.

We then determined the top full models for predicting Rt (or Rt_{ARIMA}). To do so, we compared models with all possible combinations of candidate variables, including $ln[H]$*$ln[TWI]$ and species traits as specified above. We identified the full set of models within ΔAICc=2 of the best model (that with lowest AICc). When a variable appeared in all of these models and the sign of the coefficient was consistent across models, we viewed this as support for the acceptance/rejection of the associated prediction (Table 1). If the variable appeared in some but not all of these models, and its sign was consistent across models, we considered this partial support/rejection. In presentation of the results below, we note instances where the Rt_{ARIMA} model disagreed with the Rt model, but otherwise do not discuss the Rt_{ARIMA} model. Visualization of the best mixed effects model per drought scenario (Fig. **4**) was created by the visreg package (Breheny and Burchett, 2020).

All analysis beyond basic data collection was performed using R version 3.6.2 (R Core Team, 2019). Other R-packages used in analyses are listed in the Supplementary Information (Appendix S1). All data, code, and results are available through the SCBI-ForestGEO organization on GitHub (https://github.com/SCBI-ForestGEO: SCBI-ForestGEO-Data and McGregor_climate-sensitivity-variation repositories), with static versions corresponding to data and analyses presented here archived in Zenodo (DOIs: 10.5281/zenodo.3604993 and *[TBD]*, respectively.

Results

Tree height and microenvironment

In the years for which we have vertical profiles in climate data (2016-2018), taller trees–or those in dominant crown positions– were generally exposed to higher evaporative demand during the peak growing season months (May-August; Fig. **2**). Specifically, maximum daily wind speeds were significantly higher above the top of the canopy (40-50m) than within and below (10-30m) (Fig. **2a**). Relative humidity was also somewhat lower during June-August, ranging from ~50-80% above the canopy and ~60-90% in the understory (Fig. **2b**). Air temperature did not vary consistently across the vertical profile (Fig. **2c**).

Crown position varied as expected with height (dominant > co-dominant > intermediate > suppressed), but with substantial variation (Fig. **2d**). There were significant differences in height across all crown position classes (Fig. **2d**). A comparison test between height and crown position data from the most recent ForestGEO census (2018) revealed a correlation of 0.73.

Community-level drought responses

At the community level, cored trees showed substantial growth reductions in all three droughts, with a mean Rt of 0.86 in 1966 and 1999, and 0.84 in 1977 (Fig. **2b**). Across the entire study period (1950-2009), the focal drought years were the three years with the largest fraction of trees exhibiting $Rt \leq 0.7$. Specifically, in each drought, roughly 30% of the cored trees had growth reductions of $\geq$ 30% ($Rt \leq 0.7$): 29% in 1966, 32% in 1977, and 27% in 1999. However, some individuals exhibited increased growth, *i.e.*, $Rt > 1.0$: 26% of trees in 1966, 22% in 1977, and 26% in 1999.

In the context of the multivariate model, Rt did not vary across drought years. That is, drought year as a variable did not appear in any of the top models – *i.e.*, models that were statistically indistinguishable (ΔAICc<2) from the best model.

Tree height, microenvironment, and drought resistance

Taller trees (based on H in the drought year) showed stronger growth reductions during drought (Table 1; Figs. **4, S6**). Specifically, $ln[H]$ appeared, with a negative coefficient, in the best model ((ΔAICc=0) and all top models when evaluating the three drought years together (Tables S6-S7). The same held true for 1966 individually. For the 1977 drought, $ln[H]$ did not appear in the best model, but was included, with a negative coefficient, among the top models–*i.e.*, models that were statistically indistinguishable (ΔAICc<2) from the best model (Tables 1, S6-S7). For the 1999 drought, $ln[H]$ had no significant effect.

Rt had a significantly negative response to $ln[TWI]$ across all drought years combined (Figs. **4, S6**, Table S6-S7). The effect was also significant for 1977 and 1999 individually (Fig. **4**, Table S6). When Rt_{ARIMA} was used as the response variable, the effect was significant in 1977, and included in some of the top models in 1966 and 1999 (Table S7). This negates the idea that trees in moist microsites would be less affected by

drought. Nevertheless, we tested for a $ln[H] * ln[TWI]$ interaction, a negative sign of which could indicate that smaller trees (presumably with smaller rooting volume) are more susceptible to drought in drier microenvironments with a deeper water table. This hypothesis was rejected, as the $ln[H] * ln[TWI]$ interaction was never significant, and had a positive sign in any top models in which it appeared (Tables 1, S6-S7). This term did appear with a positive coefficient in the best Rt_{ARIMA} model for all years combined (Table S7), indicating that the negative effect of height on Rt was significantly stronger in wetter microhabitats.

Species' traits and drought resistance

Species, as a factor in ANOVA, had significant influence ($p<0.05$) on all traits (wood density, LMA, PLA_{dry}, and π_{tlp}), with more significant pairwise differences for wood density and PLA_{dry} than for LMA and π_{tlp} (Table 2, Fig. **S4** as characterized by the agricolae package de Mendiburu (2020)). Drought resistance also varied across species, overall and in each drought year (Fig. **3**). Significant differences in Rt across species were most pronounced in 1966 with a total of seven distinct groupings, while 1977 had four and 1999 had two. Averaged across all droughts, Rt was lowest in *Liriodendron tulipifera* (mean Rt = **0.66**) and highest in *Fagus grandifolia* (mean Rt = **0.99**).

Wood density, LMA, and xylem porosity were all poor predictors of Rt (Tables 1,S4-S5). Wood density and LMA were never significantly associated with Rt in the single-variable tests and were therefore excluded from the full models. Xylem porosity was also excluded from the full models, as it had no significant influence for all droughts combined and had contrasting effects in the individual droughts: whereas ring-porous species had higher Rt than diffuse- and semi-ring- porous species in the 1966 and 1999 droughts, they had lower Rt in 1977 (Table S4). It is noteworthy that the two diffuse-porous species in our study, *Liriodendron tulipifera* and *Fagus grandifolia*, were at opposite ends of the Rt spectrum (Fig. **3**), further refuting the idea that xylem porosity is a useful predictor of Rt in the context of this study.

In contrast, PLA_{dry}, and π_{tlp} - the traits that qualified for inclusion in the full model (Table S4) - were both negatively correlated to drought resistance (Figs. **4, S6**; Tables 1,S4-S7). PLA_{dry} had a significant influence, with negative coefficient, in full models for the three droughts combined and for the 1966 drought individually (Fig. **4**; Tables S6-S7). For 1977 and 1999, it was included with a negative coefficient in some of the top models (Tables S6-S7). π_{tlp} was included with a negative coefficient in the best model for both all droughts combined and for the 1977 drought individually (Fig. **4**; Table S6). It was also included in some of the top models for 1999 (Tables S6-S7).

Discussion

Tree height, microenvironment, and leaf drought tolerance traits shaped tree growth responses across three droughts at our study site (Table 1, Fig. **4**). The greater susceptibility of larger trees to drought, similar to forests worldwide (Bennett et al., 2015), was driven primarily by their height (Stovall et al., 2019). Taller height was likely a liability in itself, and was also associated with greater exposure to conditions that would promote water loss and heat damage during drought (Fig. **2**). There was no evidence that greater availability of, or access to, soil water availability increased drought resistance; in contrast, trees in wetter topographic positions had lower Rt (Zuleta et al., 2017; Stovall et al., 2019), and the larger potential rooting volume of large trees provided no advantage in the drier microenvironments. The negative effect of height on Rt held after accounting for species' traits, which is consistent with recent work finding height had a stronger

influence on mortality risk than forest type during drought (Stovall et al., 2020). Drought resistance was not consistently linked to species' LMA, wood density, or xylem type (ring- vs. diffuse porous), but was negatively correlated with leaf drought tolerance traits (PLA_{dry}, π_{tlp}). This is the first study to our knowledge linking PLA_{dry} and π_{tlp} to growth reduction during drought. The directions of these responses were consistent across droughts (Table S6), supporting the premise that they were driven by fundamental physiological mechanisms. However, the strengths of each predictor varied across droughts (Fig. **4**; Tables S6-S7), indicating that drought characteristics interact with tree size, microenvironment, and traits to shape which individuals are most affected. These findings advance our knowledge of the factors that make trees vulnerable to growth declines during drought and, by extension, likely make them more vulnerable to mortality (Sapes et al., 2019).

The droughts considered here were of a magnitude that has occurred with an average frequency of approximately once every 10-15 years (Fig. **1a**, Helcoski et al., 2019) and had substantial but not devastating impacts on tree growth (Figs. **1b**). These droughts were classified as severe ($PDSI$ < -3.0; 1977) or extreme ($PDSI$ < -4.0; 1966, 1999) at our site and have been linked to tree mortality in the eastern United States (Druckenbrod et al., 2019). However, extreme, multiannual droughts such as the so-called "megadroughts" of this type that have triggered massive tree die-off in other regions (e.g., Allen et al., 2010; Stovall et al., 2019) have not occurred in the Eastern United States within the past several decades (Clark et al., 2016). Of the droughts considered here, the 1966 drought, which was preceded by two years of dry conditions (Fig. **S1**), severely stressed a larger portion of trees (Fig. **1b**). The tendency for large trees to have lowest resistance was most pronounced in this drought, consistent with other findings that this physiological response increases with drought severity (Bennett et al., 2015; Stovall et al., 2019). Across all three droughts, the majority of trees experienced reduced growth, but a substantial portion had increased growth (Fig. **1b**), consistent with prior observations that smaller trees can exhibit increased growth rates during drought (Bennett et al., 2015). It is likely because of the moderate impact of these droughts, along with other factors influencing tree growth (e.g., stand dynamics), that our best models characterize only a modest amount of variation in Rt: 11-12% for all droughts combined, and 18-25% for each individual drought (Fig. **S6**; Table S6).

Consistent with studies in other forests worldwide (Bennett et al., 2015), taller trees in this forest exhibited lower drought resistance. Mechanistically, this is consistent with, and reinforces, previous findings that biophysical constraints make it impossible for trees to efficiently transport water to great heights and simultaneously maintain strong resistance and resilience to drought-induced embolism (Olson et al., 2018; Couvreur et al., 2018; Roskilly et al., 2019). Taller trees also face dramatically different microenvironments (Fig. **2**). They are exposed to higher wind speeds and lower humidity (Fig. **2a-b**), resulting in higher evaporative demand. Unlike other temperate forests where modestly cooler understory conditions have been documented (Zellweger et al., 2019), particularly under drier conditions (Davis et al., 2019), we observed no significant variation in air temperatures across the vertical profile (Fig. **2c**). More critically for tree physiology, leaf temperatures can become significantly elevated over air temperature under conditions of high solar radiation and low stomatal conductance (Campbell and Norman, 1998; Rey-Sánchez et al., 2016). Under drought, when air temperatures tend to be warmer, direct solar radiation tends to be higher (because of less cloud cover), and less water is available for evaporative cooling of the leaves, trees with sun-exposed crowns may not be able to simultaneously maintain leaf temperatures below damaging extremes and avoid drought-induced embolism. Indeed, previous studies have shown lower drought resistance in more exposed trees (Liu and Muller, 1993; Suarez et al., 2004; Scharnweber et al., 2019). Unfortunately, collinearity

between height and crown exposure in this study (Fig. **2d**) makes it impossible to confidently partition causality. Additional research comparing drought responses of early successional and mature forest stands, along with short and tall isolated trees, would be valuable for more clearly disentangling the roles of tree height and crown exposure.

Belowground, taller trees would tend to have larger root systems (Enquist and Niklas, 2002), but this does not necessarily imply that they have greater access to or reliance on deep soil-water resources that may be critical during drought. While tree size can correlate with the depth of water extraction (Brum et al., 2019), the linkage is not consistent. Shorter trees can vary broadly in the depth of water uptake (Stahl et al., 2013), and larger trees may allocate more to abundant shallow roots that are beneficial for taking up water from rainstorms (Meinzer et al., 1999). Moreover, reliance on deep soil-water resources can actually prove a liability during severe and prolonged drought, as these can experience more intense water scarcity relative to non-drought conditions (Chitra-Tarak et al., 2018). In any case, the potentially greater access to water did not override the disadvantage conferred by height–and, in fact, greater moisture access in non-drought years (here, higher TWI) appears to make trees more sensitive to drought (Zuleta et al., 2017; Stovall et al., 2019). This may be because moister habitats would tend to support species and individuals with more mesophytic traits (Bartlett et al., 2016b; Mencuccini, 2003; Medeiros et al., 2019), potentially growing to greater heights [e.g., Detto et al. (2013), and these are then more vulnerable when drought hits. The observed height-sensitivity of *Rt*, together with the lack of conferred advantage to large stature in drier topographic positions, agrees with the concept that physiological limitations to transpiration under drought shift from soil water availability to the plant-atmosphere interface as forests age (Bretfeld et al., 2018), such that tall, dominant trees are the most sensitive in mature forests. Again, additional research comparing drought responses across forests with different tree heights and water availability would be valuable for disentangling the relative importance of above- and belowground mechanisms across trees of different size.

The development of tree-ring chronologies for the twelve most dominant tree species at our site (Helcoski et al., 2019; Bourg et al., 2013) gave us the sample size to compare historical drought responses across species (Fig. **3**) and associated traits at a single site (see also Elliott et al., 2015). Our study reinforced current understanding (see Introduction) that wood density and LMA are not reliably linked to drought resistance (Table 1). Contrary to several previous studies in temperate deciduous forests (Friedrichs et al., 2009; Elliott et al., 2015; Kannenberg et al., 2019), we did not find an association between xylem porosity and drought resistance, as the two diffuse-porous species, *Liriodendron tulipifera* and *Fagus grandifolia*, were at opposite ends of the *Rt* spectrum (Fig. **3**). While the low *Rt* of *L. tulipifera* is consistent with other studies (Elliott et al., 2015), the high *Rt* of *F. grandifolia* contrasts with studies identifying diffuse porous species in general (Elliott et al., 2015; Kannenberg et al., 2019), and the genus *Fagus* in particular (Friedrichs et al., 2009), as drought sensitive. There are two potential explanations for this discrepancy. First, other traits can and do override the influence of xylem porosity on drought resistance. Ring-porous species are restricted mainly to temperate deciduous forests, while highly drought-tolerant diffuse-porous species exist in other biomes (Wheeler et al., 2007). *Fagus grandifolia* had intermediate π_{tlp} and low PLA_{dry} (Fig. **S4**), which would have contributed to its drought resistance (Fig. **4**; see discussion below). A second explanation of why *F. grandifolia* trees at this particular site had higher *Rt* is that the sampled individuals, reflective of the population within the plot, are generally shorter and in less-dominant canopy positions compared to most other species (Fig. **S4**). The species, which is highly shade-tolerant, also has deep crowns (Anderson-Teixeira et al., 2015b), implying that a lower proportion of leaves would be affected by harsher

microclimatic conditions at the top of the canopy under drought (Fig. **2**). Thus, the high *Rt* of the sampled *F. grandifolia* population can be explained by a combination of fairly drought-resistant leaf traits, shorter stature, and a buffered microenvironment.

Concerted measurement of tree-rings and leaf drought tolerance traits of emerging importance (Scoffoni et al., 2014; Bartlett et al., 2016a; Medeiros et al., 2019) allowed novel insights into the role of drought tolerance traits in shaping drought response. The finding that PLA_{dry} and π_{tlp} can be useful for predicting drought responses of tree growth (Fig. **4**; Table 1) is both novel and consistent with previous studies linking these traits to habitat and drought tolerance. Previous studies have demonstrated that π_{tlp} and PLA_{dry} are physiologically meaningful traits linked to species distribution along moisture gradients (Maréchaux et al., 2015; Fletcher et al., 2018; Medeiros et al., 2019; Simeone et al., 2019; Rosas et al., 2019; Zhu et al., 2018), and our findings indicate that these traits also influence drought responses. Furthermore, the observed linkage of π_{tlp} to *Rt* in this forest aligns with observations in the Amazon that π_{tlp} is higher in drought-intolerant than drought-tolerant plant functional type. Further, it adds support to the idea that this trait is useful for categorizing and representing species' drought responses in models (Powell et al., 2017). Because both PLA_{dry} and π_{tlp} can be measured relatively easily (Bartlett et al., 2012; Scoffoni et al., 2014), they hold promise for predicting drought growth responses across diverse forests. The importance of predicting drought responses from species traits increases with tree species diversity; whereas it is feasible to study drought responses for all dominant species in most boreal and temperate forests (e.g., this study), this becomes difficult to impossible for species that do not form annual rings, and for diverse tropical forests. Although progress is being made for the tropics (Schöngart et al., 2017), a full linkage of drought tolerance traits to drought responses would be invaluable for forecasting how little-known species and whole forests will respond to future droughts (Christoffersen et al., 2016; Powell et al., 2017).

As climate change drives increasing drought in many of the world's forests (Trenberth et al., 2014; Intergovernmental Panel on Climate Change, 2015), the fate of forests and their climate feedbacks will be shaped by the biophysical and physiological drivers observed here. Our results show that taller, more exposed trees and species with less drought-tolerant leaf traits will be most affected, at least in terms of growth during the drought year. Resilience and survival are both linked to resistance (DeSoto et al., 2020; Gessler et al., 2020), implying that the same factors may influence these. Indeed, while the influence of PLA_{dry} and π_{tlp} on drought resilience and survival remains to be tested, taller trees have lower resilience (Trugman et al., 2018; Gillerot et al., 2020) and survival (Bennett et al., 2015; Stovall et al., 2019). As climate change-driven droughts affect forests worldwide, there is likely to be a shift from mature forests with tall, buffering trees to forests with a shorter overall stature (McDowell et al., 2020). At this point, species whose drought resistance relies in part on existence within a buffered microenvironment (e.g., *F. grandifolia*) could in turn become more susceptible. Here, the relative importance of tree height *per se* versus crown exposure becomes crucial, shaping whether the dominant trees of shorter canopies are significantly more drought resistant because of their shorter stature, or whether high exposure makes them as vulnerable as the taller trees of the former canopy. Studies disentangling the influence of height and exposure on drought tolerance will be critical to answering this question. Ultimately, distributions of tree heights and drought tolerance traits across broad moisture gradients suggest that forests exposed to more drought will shift towards shorter stature and be dominated by species with more drought-tolerant traits (Liu et al., 2019; Bartlett et al., 2016a; Zhu et al., 2018). Our study helps to elucidate the mechanisms behind these patterns, opening the door for more accurate forecasting of forest responses to future drought.

Acknowledgements

We especially thank the numerous researchers who helped to collect the data used here, in particular Jennifer C. McGarvey, Jonathan R. Thompson, and Victoria Meakem for original collection and processing of cores. Thanks also to Camila D. Medeiros for guidance on leaf drought tolerance and functional trait measurements, Edward Brzostek's lab for collaboration on leaf sampling, and Maya Prestipino for data collection. This manuscript was improved based on helpful reviews by Mark Olson and three anonymous reviewers. Funding for the establishment of the SCBI ForestGEO Large Forest Dynamics Plot was provided by the Smithsonian-led Forest Global Earth Observatory (ForestGEO), the Smithsonian Institution, and the HSBC Climate Partnership. This study was funded by ForestGEO, a Virginia Native Plant Society grant to KAT and AJT, and support from the Harvard Forest and National Science Foundation which supports the PalEON project (NSF EF-1241930) for NP.

Author Contribution

KAT, IM, and AJT designed the research. Tree-ring chronologies were developed by RH under guidance of AJT and NP. Trait data were collected by IM, JZ under guidance of NK and LS. Other plot data were collected by IM, AS, EGA, and NB under guidance of EGA and WM. Data analyses were performed by IM under guidance of KAT and VH. KAT and IM interpreted the results. IM and KAT wrote the first draft of manuscript, and all authors contributed to revisions.

Supplementary Information

Table S1. Monthly Palmer Drought Severity Index (PDSI), and its rank among all years between 1950 and 2009 (driest=1), for focal droughts.

Table S2. Species-specific bark thickness regression equations.

Table S3. Species-specific height regression equations.

Table S4. Individual tests of species traits as drivers of drought resistance, where Rt is used as the response variable.

Table S5. Individual tests of species traits as drivers of drought resistance, where Rt_{ARIMA} is used as the response variable.

Table S6. Summary of top full models for each drought instance, where Rt is used as the response variable.

Table S7. Summary of top models for each drought instance, where Rt_{ARIMA} is used as the response variable.

Figure S1. Time series of Palmer Drought Severity Index (PDSI) for the 2.5 years prior to each focal drought

Figure S2. Map of ForestGEO plot showing topographic wetness index and location of cored trees

Figure S3. Distribution of reconstructed tree heights across drought years.

Figure S4. Distribution of independent variables by species.

Figure S5. Comparison of Rt and Rt_{ARIMA} results, with residuals, for each drought scenario

Figure S6. Visualization of best model, with data, for all droughts combined.

Appendix S1. Further Package Citations

References

Abrams, M. D. (1990). Adaptations and responses to drought in Quercus species of North America. *Tree Physiology*, 7(1-2-3-4):227–238.

Allen, C. D., Breshears, D. D., and McDowell, N. G. (2015). On underestimation of global vulnerability to tree mortality and forest die-off from hotter drought in the Anthropocene. *Ecosphere*, 6(8):art129.

Allen, C. D., Macalady, A. K., Chenchouni, H., Bachelet, D., McDowell, N., Vennetier, M., Kitzberger, T., Rigling, A., Breshears, D. D., Hogg, E. H. T., Gonzalez, P., Fensham, R., Zhang, Z., Castro, J., Demidova, N., Lim, J.-H., Allard, G., Running, S. W., Semerci, A., and Cobb, N. (2010). A global overview of drought and heat-induced tree mortality reveals emerging climate change risks for forests. *Forest Ecology and Management*, 259(4):660–684.

Anderegg, W. R. L., Klein, T., Bartlett, M., Sack, L., Pellegrini, A. F. A., Choat, B., and Jansen, S. (2016). Meta-analysis reveals that hydraulic traits explain cross-species patterns of drought-induced tree mortality across the globe. *Proceedings of the National Academy of Sciences*, 113(18):5024–5029.

Anderson-Teixeira, K. J., Davies, S. J., Bennett, A. C., Gonzalez-Akre, E. B., Muller-Landau, H. C., Wright, S. J., Salim, K. A., Zambrano, A. M. A., Alonso, A., Baltzer, J. L., Basset, Y., Bourg, N. A., Broadbent, E. N., Brockelman, W. Y., Bunyavejchewin, S., Burslem, D. F. R. P., Butt, N., Cao, M., Cardenas, D., Chuyong, G. B., Clay, K., Cordell, S., Dattaraja, H. S., Deng, X., Detto, M., Du, X., Duque, A., Erikson, D. L., Ewango, C. E. N., Fischer, G. A., Fletcher, C., Foster, R. B., Giardina, C. P., Gilbert, G. S., Gunatilleke, N., Gunatilleke, S., Hao, Z., Hargrove, W. W., Hart, T. B., Hau, B. C. H., He, F., Hoffman, F. M., Howe, R. W., Hubbell, S. P., Inman-Narahari, F. M., Jansen, P. A., Jiang, M., Johnson, D. J., Kanzaki, M., Kassim, A. R., Kenfack, D., Kibet, S., Kinnaird, M. F., Korte, L., Kral, K., Kumar, J., Larson, A. J., Li, Y., Li, X., Liu, S., Lum, S. K. Y., Lutz, J. A., Ma, K., Maddalena, D. M., Makana, J.-R., Malhi, Y., Marthews, T., Serudin, R. M., McMahon, S. M., McShea, W. J., Memiaghe, H. R., Mi, X., Mizuno, T., Morecroft, M., Myers, J. A., Novotny, V., Oliveira, A. A. d., Ong, P. S., Orwig, D. A., Ostertag, R., Ouden, J. d., Parker, G. G., Phillips, R. P., Sack, L., Sainge, M. N., Sang, W., Sri-ngernyuang, K., Sukumar, R., Sun, I.-F., Sungpalee, W., Suresh, H. S., Tan, S., Thomas, S. C., Thomas, D. W., Thompson, J., Turner, B. L., Uriarte, M., Valencia, R., Vallejo, M. I., Vicentini, A., Vrška, T., Wang, X., Wang, X., Weiblen, G., Wolf, A., Xu, H., Yap, S., and Zimmerman, J. (2015a). CTFS-ForestGEO: a worldwide network monitoring forests in an era of global change. *Global Change Biology*, 21(2):528–549.

Anderson-Teixeira, K. J., McGarvey, J. C., Muller-Landau, H. C., Park, J. Y., Gonzalez-Akre, E. B., Herrmann, V., Bennett, A. C., So, C. V., Bourg, N. A., Thompson, J. R., McMahon, S. M., and McShea, W. J. (2015b). Size-related scaling of tree form and function in a mixed-age forest. *Functional Ecology*, 29(12):1587–1602.

Bartlett, M. K., Klein, T., Jansen, S., Choat, B., and Sack, L. (2016a). The correlations and sequence of plant stomatal, hydraulic, and wilting responses to drought. *Proceedings of the National Academy of Sciences*, 113(46):13098–13103.

Bartlett, M. K., Scoffoni, C., Ardy, R., Zhang, Y., Sun, S., Cao, K., and Sack, L. (2012). Rapid determination of comparative drought tolerance traits: using an osmometer to predict turgor loss point. *Methods in Ecology and Evolution*, 3(5):880–888.

Bartlett, M. K., Zhang, Y., Yang, J., Kreidler, N., Sun, S.-W., Lin, L., Hu, Y.-H., Cao, K.-F., and Sack, L. (2016b). Drought tolerance as a driver of tropical forest assembly: resolving spatial signatures for multiple processes. *Ecology*, 97(2):503–514.

Bates, D., Maechler, M., Bolker, B., and Walker, S. (2019). *lme4: Linear Mixed-Effects Models using 'Eigen' and S4*. R package version 1.1-21.

Bennett, A. C., McDowell, N. G., Allen, C. D., and Anderson-Teixeira, K. J. (2015). Larger trees suffer most during drought in forests worldwide. *Nature Plants*, 1(10):15139.

Beven, K. J. and Kirkby, M. J. (1979). A physically based, variable contributing area model of basin hydrology / Un modèle à base physique de zone d'appel variable de l'hydrologie du bassin versant. *Hydrological Sciences Bulletin*, 24(1):43–69.

Bonan, G. B. (2008). Forests and Climate Change: Forcings, Feedbacks, and the Climate Benefits of Forests. *Science*, 320(5882):1444–1449.

Bourg, N. A., McShea, W. J., Thompson, J. R., McGarvey, J. C., and Shen, X. (2013). Initial census, woody seedling, seed rain, and stand structure data for the SCBI SIGEO Large Forest Dynamics Plot. *Ecology*, 94(9):2111–2112.

Breheny, P. and Burchett, W. (2020). *visreg: Visualization of Regression Models*. R package version 2.7.0.1.

Bretfeld, M., Ewers, B. E., and Hall, J. S. (2018). Plant water use responses along secondary forest succession during the 2015–2016 El Niño drought in Panama. *New Phytologist*, 219(3):885–899.

Brewer, M. J., Butler, A., and Cooksley, S. L. (2016). The relative performance of AIC, AICC and BIC in the presence of unobserved heterogeneity. *Methods in Ecology and Evolution*, 7(6):679–692.

Brum, M., Vadeboncoeur, M. A., Ivanov, V., Asbjornsen, H., Saleska, S., Alves, L. F., Penha, D., Dias, J. D., Aragão, L. E. O. C., Barros, F., Bittencourt, P., Pereira, L., and Oliveira, R. S. (2019). Hydrological niche segregation defines forest structure and drought tolerance strategies in a seasonal Amazon forest. *Journal of Ecology*, 107(1):318–333.

Campbell, G. S. and Norman, J. M. (1998). *An Introduction to Environmental Biophysics*, volume 2nd. Springer, New York.

Chitra-Tarak, R., Ruiz, L., Dattaraja, H. S., Kumar, M. S. M., Riotte, J., Suresh, H. S., McMahon, S. M., and Sukumar, R. (2018). The roots of the drought: Hydrology and water uptake strategies mediate forest-wide demographic response to precipitation. *Journal of Ecology*, 106(4):1495–1507.

Christoffersen, B. O., Gloor, M., Fauset, S., Fyllas, N. M., Galbraith, D. R., Baker, T. R., Kruijt, B., Rowland, L., Fisher, R. A., Binks, O. J., Sevanto, S., Xu, C., Jansen, S., Choat, B., Mencuccini, M., McDowell, N. G., and Meir, P. (2016). Linking hydraulic traits to tropical forest function in a size-structured and trait-driven model (TFS v.1-Hydro).

Clark, J. S., Iverson, L., Woodall, C. W., Allen, C. D., Bell, D. M., Bragg, D. C., D'Amato, A. W., Davis, F. W., Hersh, M. H., Ibanez, I., Jackson, S. T., Matthews, S., Pederson, N., Peters, M., Schwartz, M. W.,

Waring, K. M., and Zimmermann, N. E. (2016). The impacts of increasing drought on forest dynamics, structure, and biodiversity in the United States. *Global Change Biology*, 22(7):2329–2352.

Condit, R. (1998). *Tropical Forest Census Plots: Methods and Results from Barro Colorado Island, Panama and a Comparison with Other Plots*. Springer Berlin Heidelberg, Berlin, Heidelberg.

Cook, B. I., Ault, T. R., and Smerdon, J. E. (2015). Unprecedented 21st century drought risk in the American Southwest and Central Plains. *Science Advances*, 1(1):e1400082.

Couvreur, V., Ledder, G., Manzoni, S., Way, D. A., Muller, E. B., and Russo, S. E. (2018). Water transport through tall trees: A vertically explicit, analytical model of xylem hydraulic conductance in stems. *Plant, Cell & Environment*, 41(8):1821–1839.

Dai, A., Zhao, T., and Chen, J. (2018). Climate Change and Drought: a Precipitation and Evaporation Perspective. *Current Climate Change Reports*, 4(3):301–312.

Davis, K. T., Dobrowski, S. Z., Holden, Z. A., Higuera, P. E., and Abatzoglou, J. T. (2019). Microclimatic buffering in forests of the future: the role of local water balance. *Ecography*, 42(1):1–11.

de Mendiburu, F. (2020). *agricolae: Statistical Procedures for Agricultural Research*. R package version 1.3-3.

DeSoto, L., Cailleret, M., Sterck, F., Jansen, S., Kramer, K., Robert, E. M. R., Aakala, T., Amoroso, M. M., Bigler, C., Camarero, J. J., Čufar, K., Gea-Izquierdo, G., Gillner, S., Haavik, L. J., Hereş, A.-M., Kane, J. M., Kharuk, V. I., Kitzberger, T., Klein, T., Levanič, T., Linares, J. C., Mäkinen, H., Oberhuber, W., Papadopoulos, A., Rohner, B., Sangüesa-Barreda, G., Stojanovic, D. B., Suárez, M. L., Villalba, R., and Martínez-Vilalta, J. (2020). Low growth resilience to drought is related to future mortality risk in trees. *Nature Communications*, 11(1):545.

Detto, M., Muller-Landau, H. C., Mascaro, J., and Asner, G. P. (2013). Hydrological Networks and Associated Topographic Variation as Templates for the Spatial Organization of Tropical Forest Vegetation. *PLOS ONE*, 8(10):e76296.

Druckenbrod, D. L., Martin-Benito, D., Orwig, D. A., Pederson, N., Poulter, B., Renwick, K. M., and Shugart, H. H. (2019). Redefining temperate forest responses to climate and disturbance in the eastern United States: New insights at the mesoscale. *Global Ecology and Biogeography*, 28(5):557–575.

Elliott, K. J., Miniat, C. F., Pederson, N., and Laseter, S. H. (2015). Forest tree growth response to hydroclimate variability in the southern Appalachians. *Global Change Biology*, 21(12):4627–4641.

Enquist, B. J. and Niklas, K. J. (2002). Global Allocation Rules for Patterns of Biomass Partitioning in Seed Plants. *Science*, 295(5559):1517–1520.

Farrell, C., Szota, C., and Arndt, S. K. (2017). Does the turgor loss point characterize drought response in dryland plants? *Plant, Cell & Environment*, 40(8):1500–1511.

Fletcher, L. R., Cui, H., Callahan, H., Scoffoni, C., John, G. P., Bartlett, M. K., Burge, D. O., and Sack, L. (2018). Evolution of leaf structure and drought tolerance in species of Californian Ceanothus. *American Journal of Botany*, 105(10):1672–1687.

Friedlingstein, P., Cox, P., Betts, R., Bopp, L., von Bloh, W., Brovkin, V., Cadule, P., Doney, S., Eby, M., Fung, I., Bala, G., John, J., Jones, C., Joos, F., Kato, T., Kawamiya, M., Knorr, W., Lindsay, K., Matthews, H. D., Raddatz, T., Rayner, P., Reick, C., Roeckner, E., Schnitzler, K.-G., Schnur, R.,

Strassmann, K., Weaver, A. J., Yoshikawa, C., and Zeng, N. (2006). Climate–Carbon Cycle Feedback Analysis: Results from the C4MIP Model Intercomparison. *Journal of Climate*, 19(14):3337–3353.

Friedrichs, D. A., Trouet, V., Büntgen, U., Frank, D. C., Esper, J., Neuwirth, B., and Löffler, J. (2009). Species-specific climate sensitivity of tree growth in Central-West Germany. *Trees*, 23(4):729.

Gessler, A., Bottero, A., Marshall, J., and Arend, M. (2020). The way back: recovery of trees from drought and its implication for acclimation. *New Phytologist*.

Gillerot, L., Forrester, D. I., Bottero, A., Rigling, A., and Lévesque, M. (2020). Tree Neighbourhood Diversity Has Negligible Effects on Drought Resilience of European Beech, Silver Fir and Norway Spruce. *Ecosystems*.

Gonzalez-Akre, E., Meakem, V., Eng, C.-Y., Tepley, A. J., Bourg, N. A., McShea, W., Davies, S. J., and Anderson-Teixeira, K. (2016). Patterns of tree mortality in a temperate deciduous forest derived from a large forest dynamics plot. *Ecosphere*, 7(12):e01595.

Greenwood, S., Ruiz-Benito, P., Martínez-Vilalta, J., Lloret, F., Kitzberger, T., Allen, C. D., Fensham, R., Laughlin, D. C., Kattge, J., Bönisch, G., Kraft, N. J. B., and Jump, A. S. (2017). Tree mortality across biomes is promoted by drought intensity, lower wood density and higher specific leaf area. *Ecology Letters*, 20(4):539–553.

Guerfel, M., Baccouri, O., Boujnah, D., Chaïbi, W., and Zarrouk, M. (2009). Impacts of water stress on gas exchange, water relations, chlorophyll content and leaf structure in the two main Tunisian olive (Olea europaea L.) cultivars. *Scientia Horticulturae*, 119(3):257–263.

Hacket-Pain, A. J., Cavin, L., Friend, A. D., and Jump, A. S. (2016). Consistent limitation of growth by high temperature and low precipitation from range core to southern edge of European beech indicates widespread vulnerability to changing climate. *European Journal of Forest Research*, 135(5):897–909.

Harris, I., Jones, P. D., Osborn, T. J., and Lister, D. H. (2014). Updated high-resolution grids of monthly climatic observations – the CRU TS3.10 Dataset. *International Journal of Climatology*, 34(3):623–642.

Helcoski, R., Tepley, A. J., Pederson, N., McGarvey, J. C., Meakem, V., Herrmann, V., Thompson, J. R., and Anderson-Teixeira, K. J. (2019). Growing season moisture drives interannual variation in woody productivity of a temperate deciduous forest. *New Phytologist*, 0(0).

Hoffmann, W. A., Marchin, R. M., Abit, P., and Lau, O. L. (2011). Hydraulic failure and tree dieback are associated with high wood density in a temperate forest under extreme drought. *Global Change Biology*, 17(8):2731–2742.

Hollister, J. (2018). *elevatr: Access Elevation Data from Various APIs*. R package version 0.2.0.

Hyndman, R., Athanasopoulos, G., Bergmeir, C., Caceres, G., Chhay, L., O'Hara-Wild, M., Petropoulos, F., Razbash, S., Wang, E., and Yasmeen, F. (2020). *forecast: Forecasting Functions for Time Series and Linear Models*. R package version 8.12.

Intergovernmental Panel on Climate Change (2015). *Climate Change 2014: Impacts, Adaptation and Vulnerability: Working Group II Contribution to the IPCC Fifth Assessment Report. Volume 2 Volume 2*. OCLC: 900892773.

Jennings, S. B., Brown, N. D., and Sheil, D. (1999). Assessing forest canopies and understorey illumination: canopy closure, canopy cover and other measures. *Forestry: An International Journal of Forest Research*, 72(1):59–74.

Kannenberg, S. A., Novick, K. A., Alexander, M. R., Maxwell, J. T., Moore, D. J. P., Phillips, R. P., and Anderegg, W. R. L. (2019). Linking drought legacy effects across scales: From leaves to tree rings to ecosystems. *Global Change Biology*, 0(ja).

Katabuchi, M. (2019). *LeafArea: Rapid Digital Image Analysis of Leaf Area*. R package version 0.1.8.

Kennedy, D., Swenson, S., Oleson, K. W., Lawrence, D. M., Fisher, R., Costa, A. C. L. d., and Gentine, P. (2019). Implementing Plant Hydraulics in the Community Land Model, Version 5. *Journal of Advances in Modeling Earth Systems*, 11(2):485–513.

Koike, T., Kitao, M., Maruyama, Y., Mori, S., and Lei, T. T. (2001). Leaf morphology and photosynthetic adjustments among deciduous broad-leaved trees within the vertical canopy profile. *Tree Physiology*, 21(12-13):951–958.

Kunert, N., Aparecido, L. M. T., Wolff, S., Higuchi, N., Santos, J. d., Araujo, A. C. d., and Trumbore, S. (2017). A revised hydrological model for the Central Amazon: The importance of emergent canopy trees in the forest water budget. *Agricultural and Forest Meteorology*, 239:47–57.

Larjavaara, M. and Muller-Landau, H. C. (2013). Measuring tree height: a quantitative comparison of two common field methods in a moist tropical forest. *Methods in Ecology and Evolution*, 4(9):793–801.

Liu, H., Gleason, S. M., Hao, G., Hua, L., He, P., Goldstein, G., and Ye, Q. (2019). Hydraulic traits are coordinated with maximum plant height at the global scale. *Science Advances*, 5(2):eaav1332.

Liu, Y. and Muller, R. N. (1993). Effect of Drought and Frost on Radial Growth of Overstory and Undesrstory Stems in a Deciduous Forest. *The American Midland Naturalist*, 129(1):19–25.

Lloret, F., Keeling, E. G., and Sala, A. (2011). Components of tree resilience: effects of successive low-growth episodes in old ponderosa pine forests. *Oikos*, 120(12):1909–1920.

Lunch, C., Laney, C., Mietkiewicz, N., Sokol, E., Cawley, K., and NEON (National Ecological Observatory Network) (2020). *neonUtilities: Utilities for Working with NEON Data*. R package version 1.3.5.

Martin-Benito, D. and Pederson, N. (2015). Convergence in drought stress, but a divergence of climatic drivers across a latitudinal gradient in a temperate broadleaf forest. *Journal of Biogeography*, 42(5):925–937.

Martin-Benito, D. and Pederson, N. (2015). Convergence in drought stress, but a divergence of climatic drivers across a latitudinal gradient in a temperate broadleaf forest. *Journal of Biogeography*, 42(5):925–937.

Maréchaux, I., Bartlett, M. K., Sack, L., Baraloto, C., Engel, J., Joetzjer, E., and Chave, J. (2015). Drought tolerance as predicted by leaf water potential at turgor loss point varies strongly across species within an Amazonian forest. *Functional Ecology*, 29(10):1268–1277.

Maréchaux, I., Saint-André, L., Bartlett, M. K., Sack, L., and Chave, J. (2019). Leaf drought tolerance cannot be inferred from classic leaf traits in a tropical rainforest. *Journal of Ecology*.

Mazerolle, M. J. and portions of code contributed by Dan Linden. (2019). *AICcmodavg: Model Selection and Multimodel Inference Based on (Q)AIC(c)*. R package version 2.2-2.

McDowell, N. G. and Allen, C. D. (2015). Darcy's law predicts widespread forest mortality under climate warming. *Nature Climate Change*, 5(7):669–672.

McDowell, N. G., Allen, C. D., Anderson-Teixeira, K., Aukema, B. H., Bond-Lamberty, B., Chini, L., Clark, J. S., Dietze, M., Grossiord, C., Hanbury-Brown, A., Hurtt, G. C., Jackson, R. B., Johnson, D. J., Kueppers, L., Lichstein, J. W., Ogle, K., Poulter, B., Pugh, T. A. M., Seidl, R., Turner, M. G., Uriarte, M., Walker, A. P., and Xu, C. (2020). Pervasive shifts in forest dynamics in a changing world. *Science*, 368(6494).

McDowell, N. G., Bond, B. J., Dickman, L. T., Ryan, M. G., and Whitehead, D. (2011). Relationships Between Tree Height and Carbon Isotope Discrimination. In Meinzer, F. C., Lachenbruch, B., and Dawson, T. E., editors, *Size- and Age-Related Changes in Tree Structure and Function*, Tree Physiology, pages 255–286. Springer Netherlands, Dordrecht.

Meakem, V., Tepley, A. J., Gonzalez-Akre, E. B., Herrmann, V., Muller-Landau, H. C., Wright, S. J., Hubbell, S. P., Condit, R., and Anderson-Teixeira, K. J. (2018). Role of tree size in moist tropical forest carbon cycling and water deficit responses. *New Phytologist*, 219(3):947–958.

Medeiros, C. D., Scoffoni, C., John, G. P., Bartlett, M. K., Inman-Narahari, F., Ostertag, R., Cordell, S., Giardina, C., and Sack, L. (2019). An extensive suite of functional traits distinguishes Hawaiian wet and dry forests and enables prediction of species vital rates. *Functional Ecology*, 33(4):712–734.

Meinzer, F. C., Andrade, J. L., Goldstein, G., Holbrook, N. M., Cavelier, J., and Wright, S. J. (1999). Partitioning of soil water among canopy trees in a seasonally dry tropical forest. *Oecologia*, 121(3):293–301.

Mencuccini, M. (2003). The ecological significance of long-distance water transport: short-term regulation, long-term acclimation and the hydraulic costs of stature across plant life forms. *Plant, Cell & Environment*, 26(1):163–182.

Metcalfe, P., Beven, K., and Freer, J. (2018). *dynatopmodel: Implementation of the Dynamic TOPMODEL Hydrological Model*. R package version 1.2.1.

NEON (2018). National Ecological Observatory Network. 2016, 2017, 2018. Data Products: DP1.00001.001, DP1.00098.001, DP1.00002.001. Provisional data downloaded from http://data.neonscience.org/ in May 2019. Battelle, Boulder, CO, USA.

Olson, M., Rosell, J. A., Martínez-Pérez, C., León-Gómez, C., Fajardo, A., Isnard, S., Cervantes-Alcayde, M. A., Echeverría, A., Figueroa-Abundiz, V. A., Segovia-Rivas, A., Trueba, S., and Vázquez-Segovia, K. (2020). Xylem vessel-diameter–shoot-length scaling: ecological significance of porosity types and other traits. *Ecological Monographs*, n/a(n/a).

Olson, M. E., Anfodillo, T., Rosell, J. A., Petit, G., Crivellaro, A., Isnard, S., León-Gómez, C., Alvarado-Cárdenas, L. O., and Castorena, M. (2014). Universal hydraulics of the flowering plants: vessel diameter scales with stem length across angiosperm lineages, habits and climates. *Ecology Letters*, 17(8):988–997.

Olson, M. E., Soriano, D., Rosell, J. A., Anfodillo, T., Donoghue, M. J., Edwards, E. J., León-Gómez, C.,

751 Dawson, T., Martínez, J. J. C., Castorena, M., Echeverría, A., Espinosa, C. I., Fajardo, A., Gazol, A.,
752 Isnard, S., Lima, R. S., Marcati, C. R., and Méndez-Alonzo, R. (2018). Plant height and hydraulic
753 vulnerability to drought and cold. *Proceedings of the National Academy of Sciences*, 115(29):7551–7556.

754 Phillips, N. G., Ryan, M. G., Bond, B. J., McDowell, N. G., Hinckley, T. M., and Čermák, J. (2003).
755 Reliance on stored water increases with tree size in three species in the Pacific Northwest. *Tree Physiology*,
756 23(4):237–245.

757 Powell, T. L., Wheeler, J. K., Oliveira, A. A. R. d., Costa, A. C. L. d., Saleska, S. R., Meir, P., and
758 Moorcroft, P. R. (2017). Differences in xylem and leaf hydraulic traits explain differences in drought
759 tolerance among mature Amazon rainforest trees. *Global Change Biology*, 23(10):4280–4293.

760 Pretzsch, H., Schütze, G., and Biber, P. (2018). Drought can favour the growth of small in relation to tall
761 trees in mature stands of Norway spruce and European beech. *Forest Ecosystems*, 5(1):20.

762 R Core Team (2019). *R: A Language and Environment for Statistical Computing*. R Foundation for
763 Statistical Computing, Vienna, Austria.

764 Rey-Sánchez, A. C., Slot, M., Posada, J. M., and Kitajima, K. (2016). Spatial and seasonal variation in leaf
765 temperature within the canopy of a tropical forest. *Climate Research*, 71(1):75–89.

766 Rosas, T., Mencuccini, M., Barba, J., Cochard, H., Saura-Mas, S., and Martínez-Vilalta, J. (2019).
767 Adjustments and coordination of hydraulic, leaf and stem traits along a water availability gradient. *New*
768 *Phytologist*, 223(2):632–646.

769 Roskilly, B., Keeling, E., Hood, S., Giuggiola, A., and Sala, A. (2019). Conflicting functional effects of xylem
770 pit structure relate to the growth-longevity trade-off in a conifer species. *PNAS. doi:*
771 */10.1073/pnas.1900734116.*

772 Ryan, M. G., Phillips, N., and Bond, B. J. (2006). The hydraulic limitation hypothesis revisited. *Plant, Cell*
773 *& Environment*, 29(3):367–381.

774 Sapes, G., Roskilly, B., Dobrowski, S., Maneta, M., Anderegg, W. R. L., Martinez-Vilalta, J., and Sala, A.
775 (2019). Plant water content integrates hydraulics and carbon depletion to predict drought-induced seedling
776 mortality. *Tree Physiology*, 39(8):1300–1312.

777 Scharnweber, T., Heinze, L., Cruz-García, R., van der Maaten-Theunissen, M., and Wilmking, M. (2019).
778 Confessions of solitary oaks: We grow fast but we fear the drought. *Dendrochronologia*, 55:43–49.

779 Scholz, F. G., Phillips, N. G., Bucci, S. J., Meinzer, F. C., and Goldstein, G. (2011). Hydraulic Capacitance:
780 Biophysics and Functional Significance of Internal Water Sources in Relation to Tree Size. In Meinzer,
781 F. C., Lachenbruch, B., and Dawson, T. E., editors, *Size- and Age-Related Changes in Tree Structure and*
782 *Function*, Tree Physiology, pages 341–361. Springer Netherlands, Dordrecht.

783 Schöngart, J., Bräuning, A., Barbosa, A. C. M. C., Lisi, C. S., and de Oliveira, J. M. (2017).
784 Dendroecological Studies in the Neotropics: History, Status and Future Challenges. In Amoroso, M. M.,
785 Daniels, L. D., Baker, P. J., and Camarero, J. J., editors, *Dendroecology: Tree-Ring Analyses Applied to*
786 *Ecological Studies*, Ecological Studies, pages 35–73. Springer International Publishing, Cham.

787 Scoffoni, C., Vuong, C., Diep, S., Cochard, H., and Sack, L. (2014). Leaf Shrinkage with Dehydration:
788 Coordination with Hydraulic Vulnerability and Drought Tolerance. *Plant Physiology*, 164(4):1772–1788.

Simeone, C., Maneta, M. P., Holden, Z. A., Sapes, G., Sala, A., and Dobrowski, S. Z. (2019). Coupled ecohydrology and plant hydraulics modeling predicts ponderosa pine seedling mortality and lower treeline in the US Northern Rocky Mountains. *New Phytologist*, 221(4):1814–1830.

Slette, I. J., Post, A. K., Awad, M., Even, T., Punzalan, A., Williams, S., Smith, M. D., and Knapp, A. K. (2019). How ecologists define drought, and why we should do better. *Global Change Biology*, 0(0):1–8.

Stahl, C., Hérault, B., Rossi, V., Burban, B., Bréchet, C., and Bonal, D. (2013). Depth of soil water uptake by tropical rainforest trees during dry periods: does tree dimension matter? *Oecologia*, 173(4):1191–1201.

Stovall, A. E. L., Anderson-Teixeira, K. J., and Shugart, H. H. (2018a). Assessing terrestrial laser scanning for developing non-destructive biomass allometry. *Forest Ecology and Management*, 427:217–229.

Stovall, A. E. L., Anderson-Teixeira, K. J., and Shugart, H. H. (2018b). Terrestrial LiDAR-derived non-destructive woody biomass estimates for 10 hardwood species in Virginia. *Data in Brief*, 19:1560–1569.

Stovall, A. E. L., Shugart, H., and Yang, X. (2019). Tree height explains mortality risk during an intense drought. *Nature Communications*, 10(1):1–6.

Stovall, A. E. L., Shugart, H. H., and Yang, X. (2020). Reply to "Height-related changes in forest composition explain increasing tree mortality with height during an extreme drought". *Nature Communications*, 11(1):3401.

Suarez, M. L., Ghermandi, L., and Kitzberger, T. (2004). Factors predisposing episodic drought-induced tree mortality in Nothofagus– site, climatic sensitivity and growth trends. *Journal of Ecology*, 92(6):954–966.

Sørensen, R., Zinko, U., and Seibert, J. (2006). On the calculation of the topographic wetness index: evaluation of different methods based on field observations. *Hydrology and Earth System Sciences*, 10(1):101–112.

Trenberth, K. E., Dai, A., van der Schrier, G., Jones, P. D., Barichivich, J., Briffa, K. R., and Sheffield, J. (2014). Global warming and changes in drought. *Nature Climate Change*, 4(1):17–22.

Trugman, A. T., Detto, M., Bartlett, M. K., Medvigy, D., Anderegg, W. R. L., Schwalm, C., Schaffer, B., and Pacala, S. W. (2018). Tree carbon allocation explains forest drought-kill and recovery patterns. *Ecology Letters*, 21(10):1552–1560.

Wheeler, E. A., Baas, P., and Rodgers, S. (2007). Variations In Dieot Wood Anatomy: A Global Analysis Based on the Insidewood Database. *IAWA Journal*, 28(3):229–258.

Zach, A., Schuldt, B., Brix, S., Horna, V., Culmsee, H., and Leuschner, C. (2010). Vessel diameter and xylem hydraulic conductivity increase with tree height in tropical rainforest trees in Sulawesi, Indonesia. *Flora - Morphology, Distribution, Functional Ecology of Plants*, 205(8):506–512.

Zellweger, F., Coomes, D., Lenoir, J., Depauw, L., Maes, S. L., Wulf, M., Kirby, K. J., Brunet, J., Kopecký, M., Máliš, F., Schmidt, W., Heinrichs, S., Ouden, J. d., Jaroszewicz, B., Buyse, G., Spicher, F., Verheyen, K., and Frenne, P. D. (2019). Seasonal drivers of understorey temperature buffering in temperate deciduous forests across Europe. *Global Ecology and Biogeography*, 28(12):1774–1786.

Zhu, S.-D., Chen, Y.-J., Ye, Q., He, P.-C., Liu, H., Li, R.-H., Fu, P.-L., Jiang, G.-F., and Cao, K.-F. (2018). Leaf turgor loss point is correlated with drought tolerance and leaf carbon economics traits. *Tree Physiology*, 38(5):658–663.

827 Zuleta, D., Duque, A., Cardenas, D., Muller-Landau, H. C., and Davies, S. J. (2017). Drought-induced
828 mortality patterns and rapid biomass recovery in a terra firme forest in the Colombian Amazon. *Ecology*,
829 98(10):2538–2546.

Table 1. Summary of hypotheses, corresponding specific predictions, and results.

Hypotheses & Specific Predictions	Supported?	Results
Tree size and microenvironment		
Across the forest vertical profile, taller trees are exposed to higher evaporative demand.		
Taller trees experience higher wind speeds during the peak growing season months.	yes	Fig. 2
Taller trees experience lower humidity during the peak growing season months.	yes	Fig. 2
Taller trees experience higher air temperatures during the peak growing season months.	no	Fig. 2
Taller trees have more sun-exposed crowns.	yes	Fig. 2
At least within the forest setting, taller trees are less drought resistant.		
Rt decreases with height (H).	yes	Fig. 4; Tables S6, S7
Small trees (lower root volume) in drier microhabitats have lower drought resistance.		
There is a negative interactive effect between H and topographic wetness index.	(no)	Tables S6, S7
Species traits		
Species' traits–particularly leaf drought tolerance traits–predict drought reistance.		
Wood density correlates (positively or negatively) to Rt.	-	Tables S4, S5
Leaf mass per area correlates positively to Rt.	-	Tables S4, S5
Ring-porous species have higher Rt than diffuse- or semi-ring- porous.	-	Tables S4, S5
Percent loss leaf area upon desiccation correlates negatively with Rt.	yes	Fig. 4; Tables S6, S7
Water potential at turgor loss correlates negatively with Rt.	(yes)	Fig. 4; Tables S6, S7

Parentheses indicate that the prediction was supported by one but not all of the top models (Table S6). Dash symbols indicate that the response was not significant (Table S4), or not represented in any of the top models (Table S6).

Table 2. Overview of analyzed species, listed in order of their relative contributions to woody stem productivity ($ANPP_{stem}$) in the plot, along with numbers and sizes sampled, and species traits. Variable abbreviations are as in Table 3. DBH measurements are from the most recent ForestGEO census in 2018 (live trees) or tree mortality censuses in 2016 and 2017 (trees cored dead).

			contemporary DBH (cm)		species traits (mean +/- se)				
species	% $ANPP_{stem}$	n trees	mean	range	WD ($g\,cm^{-3}$)	LMA ($g\,cm^{-2}$)	xylem porosity	π_{tlp} (Mpa)	PLA (%)
Liriodendron tulipifera (LITU)	47.1	98	36.9	10 - 100.4	0.4 ± 0.03	46.9 ± 12.4	diffuse	-1.92 ± 0.17	19.6 ± 2.06
Quercus alba (QUAL)	10.7	61	47.2	11.4 - 79.1	0.61 ± 0.02	75.8 ± 11.1	ring	-2.58 ± 0.08	8.52 ± 0.37
Quercus rubra (QURU)	10.1	69	54.9	11.1 - 148	0.62 ± 0.02	71.1 ± 6.70	ring	-2.64 ± 0.28	11.0 ± 0.84
Quercus velutina (QUVE)	7.8	77	54.1	16.0 - 114.2	0.65 ± 0.04	48.7 ± 3.30	ring	-2.39 ± 0.15	13.42 ± 0.84
Quercus montana (QUPR)	4.8	59	42.3	10.5 - 87.2	0.61 ± 0.01	71.8 ± 40.2	ring	-2.36 ± 0.09	11.75 ± 1.37
Fraxinus americana (FRAM)	3.8	62	35.4	6.4 - 94.7	0.56 ± 0.01	43.3 ± 4.78	ring	-2.1 ± 0.36	13.06 ± 1.06
Carya glabra (CAGL)	3.7	31	31.4	9.8 - 98.5	0.62 ± 0.04	42.8 ± 0.94	ring	-2.13 ± 0.50	21.09 ± 5.48
Juglans nigra (JUNI)	2.1	31	48.1	24.2 - 87	1.09 ± 0.09	72.1 ± 7.10	semi-ring*	-2.76 ± 0.21	24.64 ± 8.72
Carya cordiformis (CACO)	2.0	13	27.2	10.7 - 61.5	0.83 ± 0.10	45.9 ± 15.6	ring	-2.13 ± 0.45	17.22 ± 2.25
Carya tomentosa (CATO)	2.0	13	21.0	12.1 - 32.2	0.83	45.4	ring	-2.2	16.56
Fagus grandifolia (FAGR)	1.5	80	23.5	11.2 - 107.2	0.62 ± 0.03	30.7 ± 4.94	diffuse	-2.57	9.45 ± 1.25
Carya ovalis (CAOVL)	1.1	23	35.3	14.9 - 66.0	0.96 ± 0.33	47.6 ± 3.95	ring	-2.48 ± 0.04	14.8 ± 6.34

* Semi-ring porosity is intermediate between ring and diffuse. We group it with diffuse-porous species for more even division of species between categories.

Table 3. Summary of dependent and independent variables in our statistical models fo drought resistance, along with units, definitions, and sample sizes.

variable	symbol	units	description	category	n*
Dependent variables					
drought resistance	Rt	-	ratio of growth during drought year to mean growth of the 5 years prior.	-	1623
	Rt_{ARIMA}	-	ratio of growth during drought year to growth predicted by ARIMA model.	-	1654
Independent variables					
drought year	Y	-	year of drought	1966	513
				1977	543
				1999	567
height	H	m	estimated H in drought year	-	-
topographic wetness index	TWI	-	steady-state wetness index based on slope and upstream contributing area	-	-
species' traits					
wood density	WD	g cm^{-3}	dry mass of a unit volume of fresh wood	-	-
leaf mass per area	LMA	kg m^{-2}	ratio of leaf dry mass to fresh leaf area	-	-
xylem porosity		-	vessel arrangement in xylem	ring (R)	408
				semi-ring (SR)	31
				diffuse (D)	178
turgor loss point	π_{tlp}	MPa	water potential at which leaves wilt	-	-
percent loss area	PLA_{dry}	%	percent loss of leaf area upon dessication	-	-

*Sample sizes are after removal of outliers, and refer to the Rt model. Dashes indicate that the variable was available for all records.

Figure Legends

Figure 1. Climate and species-level growth responses over our study period, highlighting the three focal drougths (a) and community-wide responses (b). Time series plot (a) shows peak growing season (May-August) climate conditions and residual chronologies for each species (see Table 3 for codes). PET and PRE data were obtained from the Climatic Research Unit high-resolution gridded dataset (CRU TS v.4.01; Harris et al. 2014). Focal droughts are indicated by dashed lines, and shading indicates the pre-drought period used in calculations of the resistance metric. Figure modified from Helcoski *et al.* (2019). Density plots (b) show the distribution of resistance values for each drought.

Figure 2. Contemporary height profiles in sun exposure and growing season microclimate under non-drought conditions. Shown are average (± SD) of daily maxima and minima of (a) wind speed, (b) relative humidity (RH), and (c) air temperature (T_{air}) averaged over each month of the peak growing season (May-August) from 2016-2018. In these plots, heights are slightly offset for visualization purposes. Asterisks indicate signficant differences between the top and bottom of the height profile. Also shown is (d) tree heights by 2018 crown position, with letters indicating significance groupings. In all plots, the dashed horizontal line indicates the 95th percentile of tree heigts in the ForestGEO plot.

Figure 3. Drought resistance, Rt, across species for the three focal droughts. Species codes are given in Table 2.

Figure 4. Visualization of best models for all droughts combined and for each individual drought year. Confidence intervals were defined via bootsrapping in the bootpredictlme4 package. Model coefficients are given in Table S6.

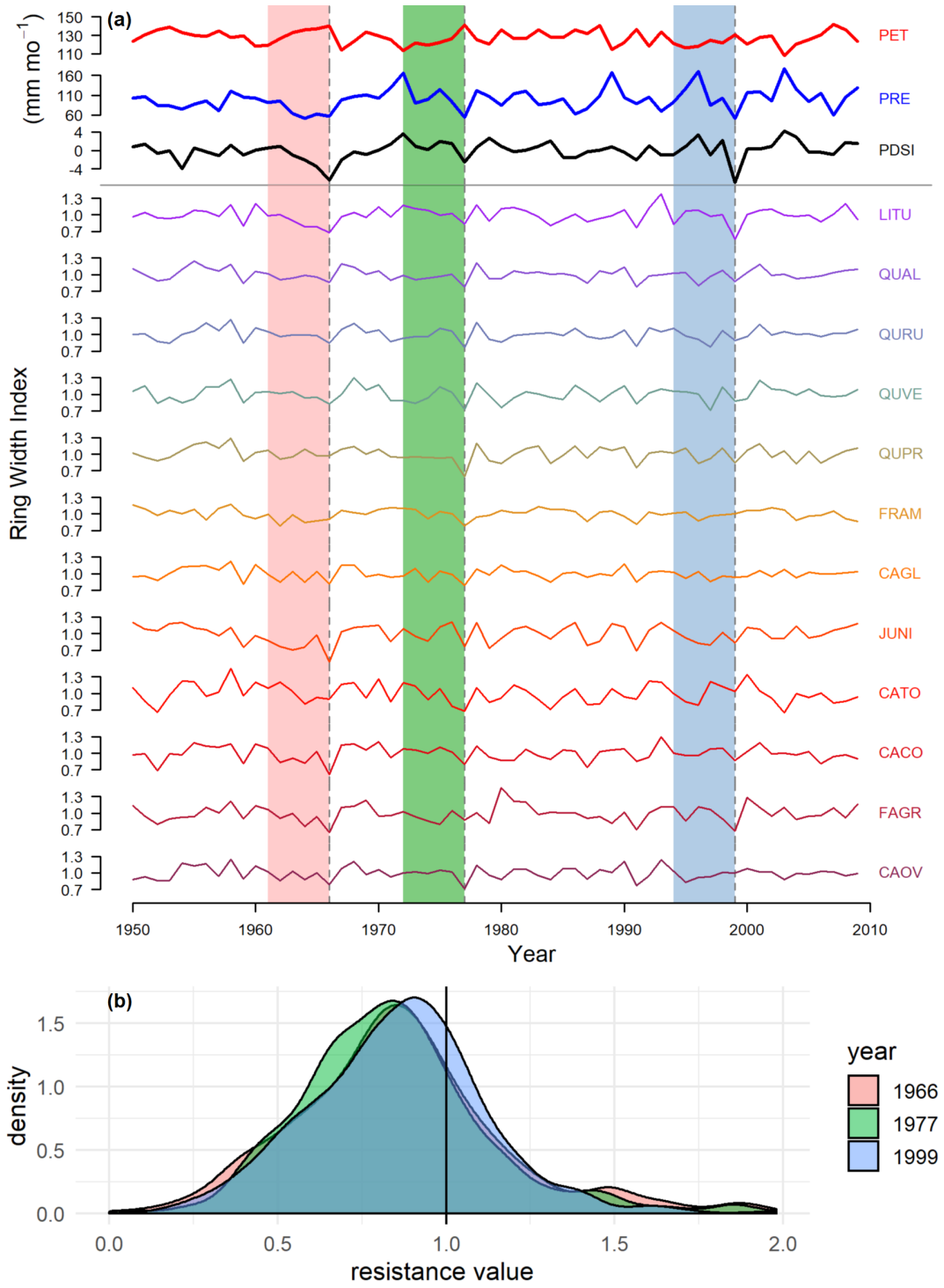

Figure 1. Climate and species-level growth responses over our study period, highlighting the three focal drougths (a) and community-wide responses (b). Time series plot (a) shows peak growing season (May-August) climate conditions and residual chronologies for each species (see Table 3 for codes). PET and PRE data were obtained from the Climatic Research Unit high-resolution gridded dataset (CRU TS v.4.01; Harris et al. 2014). Focal droughts are indicated by dashed lines, and shading indicates the pre-drought period used in calculations of the resistance metric. Figure modified from Helcoski *et al.* (2019). Density plots (b) show the distribution of resistance values for each drought.

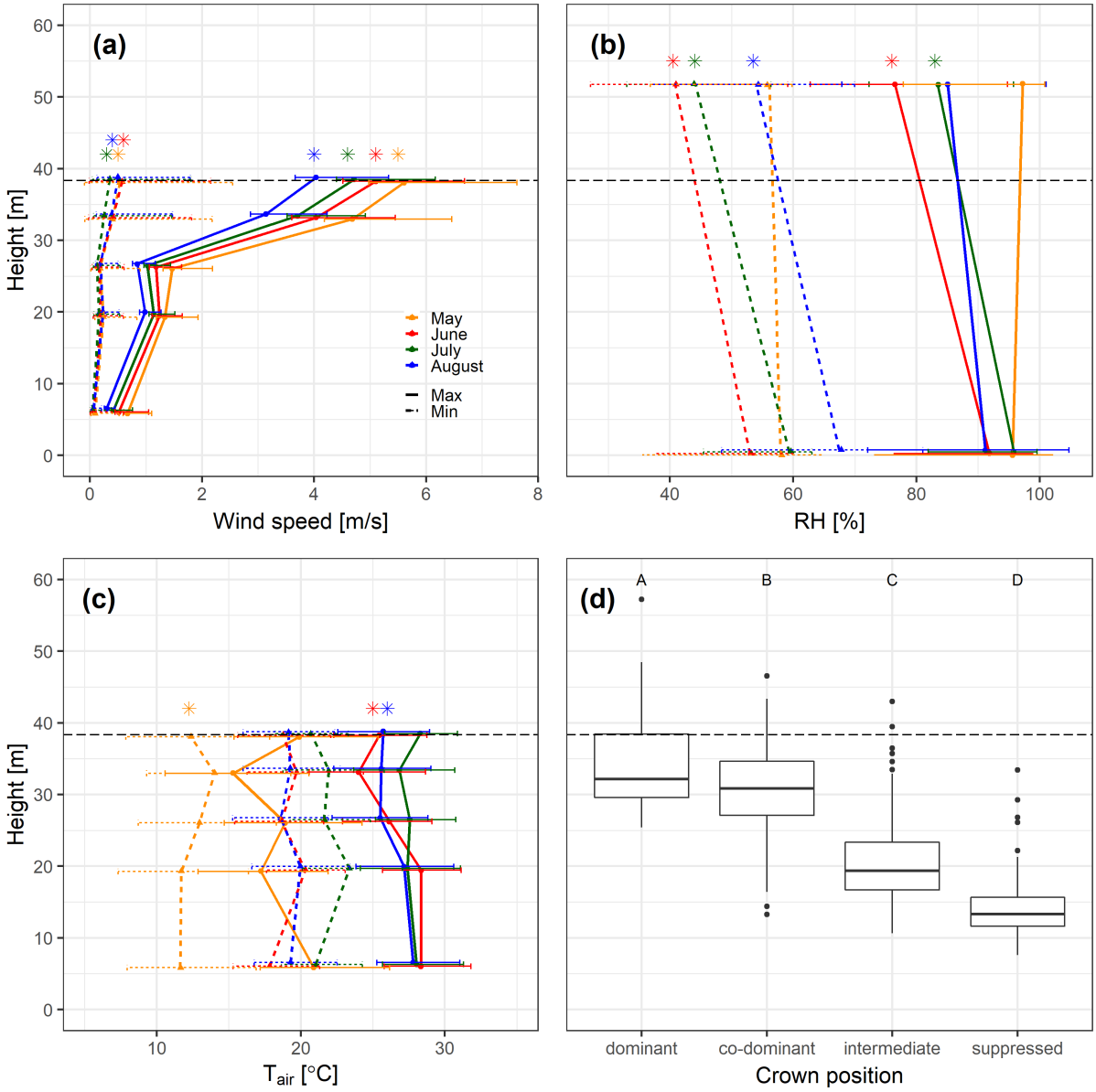

Figure 2. Contemporary height profiles in sun exposure and growing season microclimate under non-drought conditions. Shown are average (± SD) of daily maxima and minima of (a) wind speed, (b) relative humidity (RH), and (c) air temperature (T_{air}) averaged over each month of the peak growing season (May-August) from 2016-2018. In these plots, heights are slightly offset for visualization purposes. Asterisks indicate signficant differences between the top and bottom of the height profile. Also shown is (d) tree heights by 2018 crown position, with letters indicating significance groupings. In all plots, the dashed horizontal line indicates the 95th percentile of tree heigts in the ForestGEO plot.

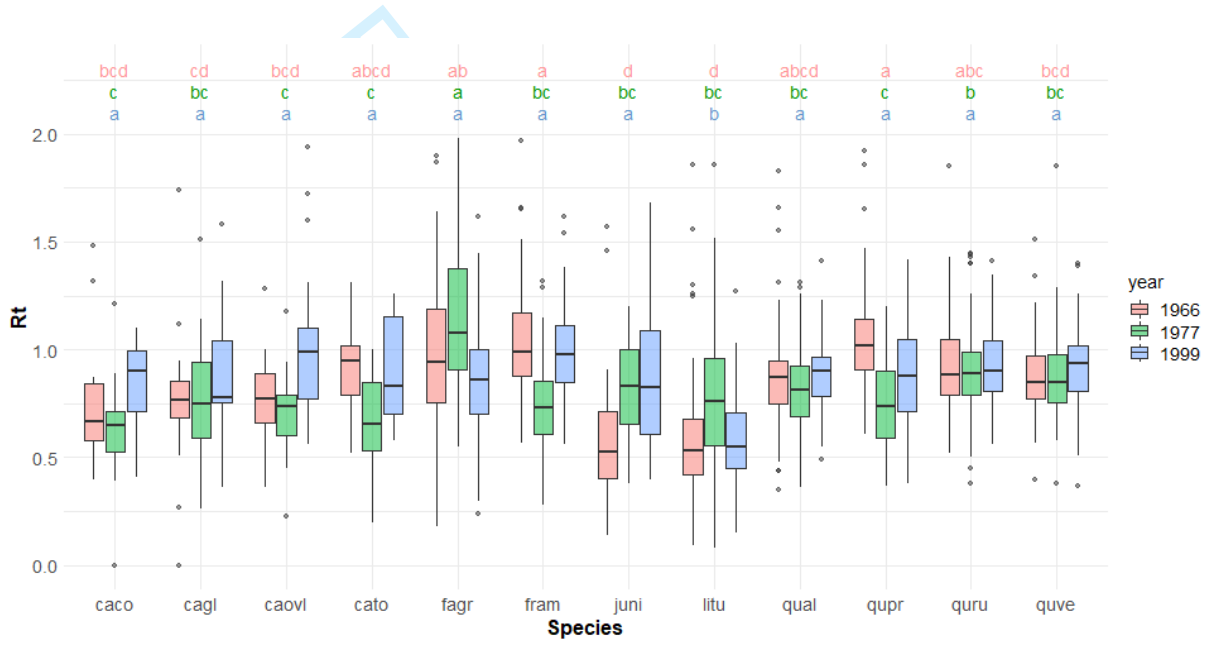

Figure 3. Drought resistance, *Rt*, across species for the three focal droughts. Species codes are given in Table 2.

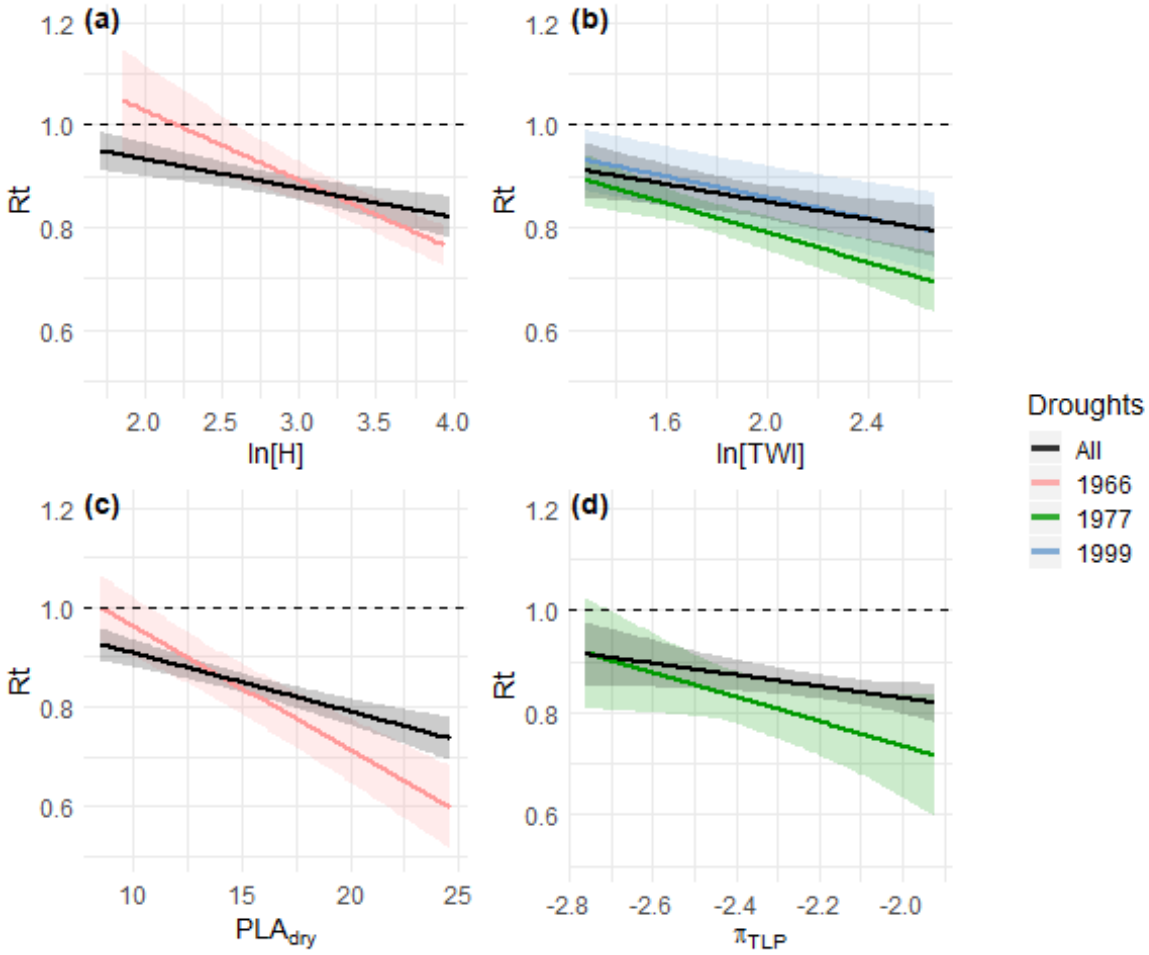

Figure 4. Visualization of best models for all droughts combined and for each individual drought year. Confidence intervals were defined via bootsrapping in the bootpredictlme4 package. Model coefficients are given in Table S6.